

Bin1 targeted immunotherapy alters the status of the enteric neurons and the microbiome during ulcerative colitis treatment

Sunil Thomas^{1*}, Giancarlo Mercogliano², George Prendergast¹

¹Lankenau Institute for Medical Research, 100 E Lancaster Ave., Wynnewood, PA-19096, USA.

²Lankenau Medical Center, Wynnewood, PA-19096.

* Email: suntom2@gmail.com

ABSTRACT

Ulcerative colitis (UC) is a common chronic disease of the large intestine. Current anti-inflammatory drugs prescribed to treat this disease have limited utility due to significant side-effects. Thus, immunotherapies for UC treatment are still sought. In the DSS mouse model of UC, we recently demonstrated that systemic administration of the Bin1 monoclonal antibody 99D (Bin1 mAb) developed in our laboratory was sufficient to reinforce intestinal barrier function and preserve an intact colonic mucosa, compared to control subjects which displayed severe mucosal lesions, high-level neutrophil and lymphocyte infiltration of mucosal and submucosal areas, and loss of crypts. Here we report effects of Bin1 mAb on colonic neurons and the gut microbiome that correlate with the benefits of treatment. In the DSS model, we found that induction of UC was associated with disintegration of enteric neurons and elevated levels of glial cells, which translocated to the muscularis at distinct sites. Further, we characterized an altered gut microbiome in DSS treated mice associated with pathogenic proinflammatory characters. Both of these features of UC induction were normalized by Bin1 mAb treatment. With regard to microbiome changes, we observed in particular that Firmicutes were eliminated by UC induction and that Bin1 mAb treatment restored this phylum including the genus *Lactobacillus* and *Akkermansia* as beneficial microorganisms. Overall, our findings suggest that the intestinal barrier function restored by Bin1 immunotherapy in the DSS model of UC is associated with a preservation of enteric neurons and an improvement in the gut microbiome, contributing overall to a healthy intestinal tract.

KEYWORDS

Ulcerative colitis, Inflammatory bowel disease, Immunotherapy, Bin1 monoclonal antibody, Enteric neurons, Microbiome, Colon.

INTRODUCTION

Ulcerative colitis (UC) is a chronic, idiopathic inflammatory bowel disease that affects the colon. UC is characterized by mucosal inflammation that starts in the rectum and often extends continuously to the proximal segments of the colon. UC usually presents with bloody diarrhea that is diagnosed by colonoscopy and histological findings (Ungaro et al. 2017). People with UC have a higher risk of developing colorectal cancer. The colorectal cancer risk is as high as 18% with 30 years of UC (Eaden et al. 2001). The increased risk of colorectal cancer is due in part to the inflammation induced loss of barrier function. As yet there are no fully effective drugs or therapies to protect against UC. The inflammatory cytokines, tumor necrosis factor (TNF)- α , and IFN- γ are elevated in UC. While anti-inflammatory drugs and immune suppressors (eg, TNF- α inhibitors) are currently prescribed for UC treatment, side effects such as the risk of opportunistic infections and the lack of efficacy in certain individuals limit the quality of treatment (Kang et al. 2018). Hence, there is an interest in developing additional immunotherapies to provide protection against UC that protects intestinal barrier.

The bridging integrator 1 (Bin1), also known as amphiphysin 2, is a nucleocytoplasmic adaptor protein with 10 isoforms. *BIN1* was initially identified in 1996 as a tumor suppressor; subsequently, however, additional functions have been attributed to different protein transcripts. Bin1 is a conserved member of the BAR (Bin-Amphiphysin-Rvs) family of adapter proteins implicated in diverse cellular processes including endocytosis, actin organization, programmed cell death, stress responses, and transcriptional control. The *BIN1* gene has recently been identified as the most important risk locus for late-onset Alzheimer's disease, after apolipoprotein E (Thomas et al. 2019b).

In a recent study, our group demonstrated that genetic attenuation of *BIN1* reduced disease severity in a mouse model of experimental colitis occurring in association with an enhancement of epithelial barrier function. On the basis of that study, we explored the ability of Bin1 monoclonal antibodies (mAb) developed by our group to phenocopy effects of genetic attenuation in the colitis model. We recently reported the development of a novel colitis therapy targeting the Bin1 protein and supporting epithelial barrier function.

We used both cell culture and animal models for the study. Mice induced with UC had severe lesions throughout the mucosa, high-level neutrophil and lymphocyte infiltration into the mucosal and submucosal areas, and loss of crypts. Whereas, animals treated with the cell penetrating Bin1 mAb protects against UC by directly improving colonic epithelial barrier function that limit gene expression and cytokine programs associated with colonic inflammation (Thomas et al. 2016; 2019a). In this paper, we report progress in how Bin1 mAb treatment protects against UC; specifically, it protects enteric neurons thereby preventing bowel movement dysfunction, and that it promotes formation of a healthy gut microbiome.

MATERIALS AND METHODS

Bin1 monoclonal antibodies. We used the therapeutic 99D Bin1 monoclonal antibody for our study (Thomas et al. 2016, 2019a, b). The antibody 99D recognizes an epitope within the C-terminal Myc binding domain encoded by exon 13 (Wechsler-Reya et al. 1997). 99D exhibited the ability to improve barrier function as demonstrated by in vitro experiments with human Caco-2 colon cells and animal models of UC (Thomas et al. 2016, 2019a).

Experimental colitis model system. For the study, we used a therapeutic animal model of UC. Animals were weighed before, during and after treatments. Briefly, male mice (C57BL/6) of 5 weeks of age were fed with 3% dextran sodium sulfate (DSS, Alfa Aesar, MW 40kDa) in drinking water ad libitum (n=5 per group). After 7 days of DSS treatment, mice were provided with distilled water. 24 hours after feeding with water they were injected i.p. (0.5 mg of purified antibody per mouse) with Bin1 mAb or antibody isotype control (Thomas et al. 2016, 2019a). After 7 days of Bin1 mAb or isotype control treatments, mice were euthanized, and colons were measured and inspected for necropsy for gross macroscopic lesions and the protein levels were determined by western blotting.

Western blot analysis. Bin1 mAb treated or control colons were dissected, and the mucosal tissue was physically scraped and lysed as previously described (Ramalingam et al. 2010). After polyacrylamide gel electrophoresis (10% gel) and transfer to nitrocellulose membrane, they were probed with antibodies for NeuN, GFAP, and VDAC (Cell Signaling, MA) according to the manufacturer's instructions.

Immunohistochemistry. The colon tissues were processed for immunohistochemistry according to Thomas et al. (2014). The tissues were probed with antibodies for NeuN, and GFAP (Cell Signaling, MA) according to the manufacturer's instructions. The cells were mounted using Fluoromount-G (Southern Biotech, AL) and visualized by confocal microscopy (Nikon Eclipse TI, Japan). Images were taken from different fields from the same slide. The experiments were repeated thrice.

Analyses of the gut microbiome. The mice were placed on a raised platform to determine the quantity of fecal pellets and urine excreted in 10 minutes. We could collect 4 to 8 fecal pellets in 10 minutes from untreated control mice. Hence, 10 minutes was maintained to monitor the fecal pellets in the treatment groups. Placing the animals on a raised platform improved fecal pellet collection compared to leaving the animals in a container for the same duration. The microbiome of the fecal pellet from the animals were analyzed directly or they were cultured in a biosimulator in Luria-Bertani (LB) medium in aerobic and anaerobic conditions. The biosimulator induce proliferation of microorganisms (Thomas, 2020). The microorganisms were cultured for 48 hours in the biosimulator, the contents pelleted in a centrifuge at 5000 g, and the samples subjected to 16S rRNA sequencing (Arizona State University Microbiome Core) for taxonomic identification. The experiments were repeated three times. Microbial DNA extraction was extracted from samples by using DNeasy PowerSoil Kit – (QIAGEN) following directions of the manufacturer.

Microbiome library preparation methodology. Bacterial community analysis was performed via next generation sequencing in MiSeq Illumina platform. Amplicon sequencing of the V4 region of the 16S rRNA gene was performed with the barcoded primer set 515f/806r designed by Caporaso et al. (2011) and following the protocol by the Earth Microbiome Project (EMP) (<http://www.earthmicrobiome.org/emp-standard-protocols/>) for the library preparation. PCR amplifications for each sample are done in triplicate, then pooled and quantified using Quant-iT™ PicoGreen® dsDNA Assay Kit (Invitrogen). A no template control sample is included during the library preparation as a control for extraneous nucleic acid contamination. 240 ng of DNA per sample are pooled and then cleaned using QIA quick PCR purification kit (QIAGEN). The pool is quantified by Illumina library Quantification Kit ABI Prism® (Kapa Biosystems). Then, the DNA pool is diluted to a final concentration of 4 nM then denatured and diluted to a final concentration of 4 pM with a 15% of PhiX. Finally, the DNA library was loaded in the MiSeq Illumina and run using the version 2 module, 2x250 paired-end, following the directions of the manufacturer.

Microbiome downstream analysis. Downstream visualization and statistics were performed by the Harvard T.H. Chan School of Public Health Microbiome Analysis Core. Briefly, samples with read counts lower than 5,000 post filtering, denoising, merging, and chimera removal were excluded from downstream analysis. Phenotypic variables were tested against the bacterial communities' alpha and beta diversity metrics, InvSimpson and Bray-Curtis dissimilarity and unweighted and weighted UniFrac distance, respectively. Alpha diversity was calculated using the estimate richness function in phyloseq (McMurdie and Holmes, 2012) and differences in diversity were found using an ANOVA test on linear models, both univariable and multivariable, and box plots were used to visualize trends. Beta diversity was calculated using the vegan (Oksanen et al. 2019) package in R and significant differences in community composition were tested using an omnibus univariable PERMANOVA test using the adonis function within the vegan package in R. Next, we incorporated covariates in multivariate models. Further, principal coordinates analysis (PCoA) plots were created on the Bray-Curtis dissimilarities and unweighted and weighted UniFrac distances. To display the samples' community compositions, stacked bar plots and heat maps on taxonomic relative abundances were constructed on the top 30 taxa and annotated with the phenotypes. All diversity trends and community composition visualizations were created using the ggplot2 package in R (Wickham, 2016).

Per-feature differences in the microbial composition were explored with the MaAsLin2 (Morgan et al. 2012) tool, which tests for statistically significant associations determined by testing each clade in a hierarchical manner after normalization from counts to relative abundances and log transforming these data. Among each of the comparisons generated, multiple comparisons are adjusted using a Benjamini and Hochberg correction and FDR corrected p-values of 0.25 or lower are reported as significant. Thus, MaAsLin2 identifies microbial organisms that reach a statistically significant association with each of the phenotypes. For all analyses other than alpha diversity, feature tables were filtered requiring a microbial feature to have at least 0.01% relative abundance in at least 10% of all samples.

Statistics. Unpaired two-tailed Student t tests were used to compare sets of data obtained from independent groups. Statistical significance was considered at the $P < 0.05$ level.

RESULTS

No statistically difference in food and liquid consumption between treatments

The mice were provided normal diet during the experiment. Equal amount of food and 3% DSS were provided to all the animals in the treatment groups. After 7 days of DSS consumption, mice were switched to regular water. Mice consumed more food and water in the second week (Fig. 1). There were no statistically significant changes in food and water consumption in the DSS treated mice in the first and second week compared to the other groups.

Phenotypic changes in mice after treatment

Mice treated with DSS alone had decrease in weight compared to the controls (Fig 2A). Bin1 mAb treated mice had increased weight compared to the DSS treated counterpart. DSS influenced the length of the colon. The colon length was longer in the untreated mice and in the Bin1 mAb treated mice compared to the mice treated with DSS (Fig. 2B).

DSS treated animals had no fecal pellets or urine after 10 minutes of monitoring on day 7. The fecal pellets and urine improved on day 14 in DSS treated animals. We demonstrated previously that Bin1 mAb immunotherapy protected against UC induction in the DSS model (Thomas et al. 2016; 2019a). In the present study, we determined that Bin1 mAb-treated animals had better counts of fecal pellets and urine compared to DSS-only or IgG-treated animals (Fig. 2C, 2D). These data argued that Bin1 mAb treatment improved bowel health in animals where UC was induced.

Changes in the enteric neurons and glial cells after induction of UC

The enteric nervous system (ENS) is the intrinsic neural network of the gastrointestinal tract that orchestrates gastrointestinal behavior independently of the central nervous system (CNS). ENS dysfunction is often linked to digestive disorders. We determined the changes in the enteric neurons after UC and during its treatment with Bin1 mAb. The protein lysate from the colon was subjected to western blotting by probing for NeuN, the enteric neuronal marker. High expression of enteric neurons was observed in the colon of untreated controls and also in the colon of the Bin1 mAb treated mice. The colon of

DSS and IgG treated mice had lower expression of NeuN, suggesting disintegration of enteric neurons during UC induction (Fig. 3A). The glial cells are known to protect the enteric neurons. We determined the status of the glial cells by western blotting. The expression of GFAP, the characteristic marker of glial cells, was higher in the colon of DSS and IgG treated mice, whereas it was lower expression in the colon of untreated control and Bin1-mAb treated mice (Fig. 3A).

To confirm the expression of enteric neurons and glial cells *in situ*, we analyzed these cells in the colon of mice by confocal microscopy. The colon of the untreated control and the Bin1 mAb treated mice had high expression of NeuN. Most of the enteric neurons were localized to the muscularis. The DSS-treated animals exhibited disintegration of enteric neurons, whereas IgG-treated animals exhibited low levels of enteric neurons (Fig. 3B). Conversely, the colon of DSS and IgG treated animals had higher expression of glial cells compared to the untreated controls or Bin1-mAb treated animals (Fig 3B). The glial cells were mostly localized to the submucosa of the colon.

The glial cells are localized in the submucosa and it is not known how they access the enteric neurons in the muscularis. The muscularis of the colon is considered a continuous entity with no openings. However, our confocal microscopy analysis revealed punctuated openings in the muscularis. Notably, glial cells were sited in these regions such that they appeared to be crossing the openings of the muscularis into the serosa layer (Fig. 4A). To confirm whether these openings are consistently present in the muscularis of the mouse, we observed the colon of mice in all the treatment groups by light microscopy after standard H&E histochemical staining. The openings were consistently seen in the muscularis of the colon in all treatment groups, further arguing that the muscularis of the colon is not a continuous entity but rather is punctuated by openings (Fig. 4B), which may enable the movement of glial cells to protect the enteric neurons.

Changes in the microbiome after induction of UC

UC etiology is not understood. One of the hypotheses is that a dysbiotic microbiome is responsible for induction of UC (Shen et al. 2018). In this study, the stool of mice before

UC, during UC and during Bin1 mAb immunotherapy or control treatments was collected for microbiome analysis. We cultured the microbiome from fecal pellets obtained from experimental subjects in a biosimulator (Thomas, 2020) under aerobic and anaerobic conditions. The bacteria had lower growth rate under anaerobic conditions. However, the bacteria multiplied rapidly under aerobic conditions. We observed the morphology of the bacteria under phase contrast microscopy. There was a drastic change in the morphology of the bacteria after the onset of UC. The untreated control animals had a heterogeneous population of bacteria. We observed single-celled and chain-like bacterial structures in the microbiome from untreated mice. However, the DSS treated animals had a homogeneous single-celled bacterial morphology. There was no change in the morphology after treatment with IgG; whereas, treatment with the Bin1 mAb influenced the morphology of the microbiome. The morphology of the bacterial cells were similar to the untreated controls demonstrating that Bin1 mAb influences the microbiome during UC treatment (Fig. 5A, B).

Subsequently, we sequenced the microbiome by 16S rRNA to understand the taxonomy of the bacteria during UC and its treatment. Notably, we observed a lack of Firmicutes during UC in the fecal pellet or when cultured in a biosimulator under aerobic and anaerobic conditions. This reduction in Firmicutes was improved during treatment with the Bin1 mAb (Fig. 6).

Data from the microbiome sequencing showed that the bacteria of the genus *Lactobacillus* was totally absent in the UC mice. *Lactobacillus* are predominantly anaerobes and levels of bacteria in this genus were elevated in subjects treated with the Bin1 mAb. (Fig 7-9) (Table 1). Likewise, *Akkermansia* is a bacterium involved in bowel health of the organism and lower levels of bacteria in this genus are related to UC (Lopez-Siles et al. 2018). In this study, we observed high levels of the *Akkermansia* in subjects treated with Bin1 mAb (Figs. 7-9) (Table 1). These data indicated that the benefits of Bin1 mAb treatment in UC were associated with favorable changes in *Lactobacillus* and *Akkermansia* consistent with potential involvement in maintaining gut health of the treated subjects where UC was induced. *Enterobacteriaceae*, *Acinetobacter*, *Bacillus* sp.,

Bifidobacterium, *Clostridiaceae*, *Achromobacter*, *Burkholderia*, *Sutterella* and *Stenotrophomonas* are also observed in the microbiome of UC in humans and animal models of the disease. In our study, we confirmed the presence of microorganisms of these various genera in the fecal pellets of DSS-treated mice, with some changes in their levels also associated with Bin1 mAb treatment (Figs. 7-9) (Table 1). Taken together, these data specified alterations in the gut microbiome that were associated with the healthful benefits of Bin1 mAb treatment in animals subjected to DSS-induced UC.

DISCUSSION

The findings of this study identify associated benefits of Bin1 mAb immunotherapy for UC treatment in preserving enteric neurons and rebalancing the gut microbiome. The identification of these effects are important, because they suggest a pleiotropic effect of Bin1 targeting in its capacity to act through multiple mechanisms to relieve UC pathophysiology.

The enteric nervous system (ENS), often referred to as a “second brain”, is large, complex and uniquely able to orchestrate gastrointestinal behavior independently of the central nervous system (CNS) (Rao and Gershon, 2016). The brain influences the ENS through sympathetic and parasympathetic nerves, but the bowel and its microbial content, through the ENS, also reciprocally affect the brain (Margolis and Gershon, 2016). The movements of the small and large intestines are controlled by the ENS. Bowel movements disrupted in UC are obstructed even if small segment of the CNS is compromised. Conversely, a lethal pseudo-obstruction occurs if even a small segment of the ENS is missing. ENS abnormalities lead to irregular bowel movements and constipation (Bassotti et al. 2011). Serotonin (5-HT) is an important neurotransmitter in the gastrointestinal tract. 95% of the body’s serotonin is produced in the intestine where it has been increasingly recognized for its hormonal, autocrine, paracrine, and endocrine actions. In the gut, a large pool of 5-HT is synthesized in the enterochromaffin (EC) cells and a smaller 5-HT pool in the ENS (Costedio et al. 2007; Li et al. 2011). There is functional difference between 5-HT synthesized by EC and ENS. Gastrointestinal motility depends more on neuronal than on mucosal 5-HT and that the development of dopaminergic, GABAergic, and calcitonin gene-related peptide (CGRP)-expressing enteric neurons requires neuronal 5-HT (Li et al. 2011).

We explored the ENS in this study because we observed that Bin1 mAb-treated animals passed more fecal pellets than control DSS-treated animals. To rule out the possibility that UC mice drink or eat little, which might explain the difference, we compared liquid and food consumption between treatments. No difference was found in the different treatment cohorts pointing to irregular bowel movements mediated by ENS as a potential

causal agent for changes in fecal pellets between groups. As expected, we found that DSS treatment disintegrated enteric neurons; however, glial cells that protect the neurons were increased. Bin1 mAb treatment positively influenced the ENS, with neurons more similar to untreated controls than DSS-treated controls. Accordingly, an intact ENS mediated by the Bin1 mAb was associated with more normal bowel movements. Although it is known that colonic glial cells protect enteric neurons, as yet we have no knowledge how the glial cells cross the muscularis where the neurons are located. However, our observations that the muscularis is not an intact continuous layer, as generally considered, may address this question via small openings (*anigma*; Greek, opening) that we observed to punctuate the colon. We propose that these *anigma* serve as a conduit for cells and molecules to transit into the muscularis.

As yet no single microorganism has been identified as an agent responsible for UC despite the large number of gut microbiome studies and the evidence supporting the claim of microbiome involvement in the pathogenesis of the disease (Knox et al. 2019). In our study, we observed that induction of UC was associated with a change in the phenotype of the bacterial population as observed by microscopy, with rebalance of the phenotype in subjects receiving Bin1 mAb treatment. These rapid changes illustrate the plasticity of the microorganismal response to an effective therapy.

Commensal *Lactobacillus* species are common inhabitants of the natural microbiota in the human gut, and by restoring homeostasis in gastrointestinal inflammatory diseases they can exert a protective role against UC (Chen et al. 2015). It has been previously shown that *Lactobacillus acidophilus* treatment can efficiently ameliorate DSS-induced experimental colitis in mice (Chen et al. (2013). In our study, we observed that *Lactobacillus* was totally absent in UC mice but restored to significant extent by Bin1 mAb treatment. Likewise, we observed that Bin1 mAb treatment increased gut levels of the genus *Akkermansia*, which is associated with a variety of health benefits including an alleviation of UC severity. In summary, our study demonstrated that the therapeutic benefits of Bin1 mAb treatment in UC mice is associated with a preservation of enteric neurons and a rebalancing of the gut microbiome. Further studies are needed to explore

the causality of these effects and whether Bin1 mAb may influence serotonin in coordinating them.

Acknowledgements

The microbiome analysis was performed at the Microbiome Core of Arizona State University. The microbiome data in this paper were handled in part through the Harvard Chan Microbiome Analysis Core by Jeremy E. Wilkinson and Chengchen Li. We express our gratitude to the Sharpe-Strumia Research Foundation, Wawa Foundation and Women's Board of Lankenau for providing grants to the project. We also acknowledge Gwendolyn Gilliard and James DuHadaway for technical assistance in the study.

Conflicts of interest

The authors declare no conflicts of interest. No writing assistance was utilized in the production of this manuscript.

Author contributions

ST conceived the study and designed the experiments. ST performed the experiments. ST, GP analyzed the data. ST wrote the manuscript. ST, GM, and GP edited the manuscript.

REFERENCES

- Bassotti G, Villanacci V, Rostami Nejad M. Chronic constipation: no more idiopathic, but a true neuropathological entity. *Gastroenterol Hepatol Bed Bench*. 2011; 4:109-115.
- Caporaso JG, Lauber CL, Walters WA, Berg-Lyons D et al. Global patterns of 16S rRNA diversity at a depth of millions of sequences per sample. *Proc. Natl Acad. Sci. USA* 2011; 108, 4516–4522.
- Chen L, Zou Y, Peng J, Lu F, Yin Y, Li F, Yang J. *Lactobacillus acidophilus* suppresses colitis-associated activation of the IL-23/Th17 axis. *J Immunol Res*. 2015; 2015:909514.
- Chen LL, Zou YY, Lu FG, Li FJ, and Lian GH. (2013). Efficacy profiles for different concentrations of *Lactobacillus acidophilus* in experimental colitis. *World Journal of Gastroenterology*, 19: 5347–5356.
- Costedio MM, Hyman N, Mawe GM. Serotonin and its role in colonic function and in gastrointestinal disorders. *Dis Colon Rectum*. 2007; 50: 376-388.
- Eaden JA, Abrams KR, Mayberry JF. The risk of colorectal cancer in ulcerative colitis: a meta-analysis. *Gut*. 2001;48(4):526-535.
- Kang J, Jeong DH, Han M, Yang SK, Byeon JS, Ye BD, Park SH, Hwang SW, Shim TS, Jo KW. Incidence of active tuberculosis within one year after tumor necrosis factor inhibitor treatment according to latent tuberculosis infection status in patients with inflammatory bowel disease. *J Korean Med Sci*. 2018; 33(47):e292.
- Knox NC, Forbes JD, Van Domselaar G, Bernstein CN. The Gut Microbiome as a Target for IBD Treatment: Are We There Yet? *Curr Treat Options Gastroenterol*. 2019; 17: 115-126.
- Lopez-Siles M, Enrich-Capó N, Aldeguer X, Sabat-Mir M, Duncan SH, Garcia-Gil LJ, Martinez-Medina M. Alterations in the Abundance and Co-occurrence of *Akkermansia muciniphila* and *Faecalibacterium prausnitzii* in the Colonic Mucosa of Inflammatory Bowel Disease Subjects. *Front Cell Infect Microbiol*. 2018; 8:281.
- Li Z, Chalazonitis A, Huang YY, Mann JJ, Margolis KG, Yang QM, Kim DO, Côté F, Mallet J, Gershon MD. Essential roles of enteric neuronal serotonin in gastrointestinal motility and the development/survival of enteric dopaminergic neurons. *J Neurosci*. 2011; 31: 8998-9009.
- Margolis KG, Gershon MD. Enteric Neuronal Regulation of Intestinal Inflammation. *Trends Neurosci*. 2016; 39: 614-624.
- McMurdie PJ, Holmes S. Phyloseq: a bioconductor package for handling and analysis of high-throughput phylogenetic sequence data. *Pac Symp Biocomput*. 2012; 235-246.

Morgan XC, Tickle TL, Sokol H, et al. Dysfunction of the intestinal microbiome in inflammatory bowel disease and treatment. *Genome Biol.* 2012;13(9):R79.

Oksanen J, Blanchet FG, Friendly M, Kindt R, Legendre P, McGlinn D, Minchin PR, O'Hara RB, Simpson GL, Solymos P, Stevens MHH, Szoecs E, Wagner H (2019). *Vegan: Community Ecology Package*. R package version 2.5-6. <https://CRAN.R-project.org/package=vegan>

Ramalingam A, Wang X, Gabello M, et al. Dietary methionine restriction improves colon tight junction barrier function and alters claudin expression pattern. *Am J Physiol Cell Physiol.* 2010; 299:C1028-C1035.

Rao M, Gershon MD. The bowel and beyond: the enteric nervous system in neurological disorders. *Nat Rev Gastroenterol Hepatol.* 2016; 13: 517-28.

Shen ZH, Zhu CX, Quan YS, Yang ZY, Wu S, Luo WW, Tan B, Wang XY. Relationship between intestinal microbiota and ulcerative colitis: Mechanisms and clinical application of probiotics and fecal microbiota transplantation. *World J Gastroenterol.* 2018; 24:5-14.

Thomas S, DuHadaway J, Prendergast GC, Laury-Kleintop L. Specific in situ detection of murine indoleamine 2, 3-dioxygenase. *J Cell Biochem.* 2014; 115: 391-396.

Thomas S, Hoxha K, Alexander W, Gilligan J, Dilbarova R, Whittaker K, Kossenkov A, Prendergast GC, Mullin JM. Intestinal barrier tightening by a cell-penetrating antibody to Bin1, a candidate target for immunotherapy of ulcerative colitis. *J Cell Biochem.* 2019a; 120:4225-4237.

Thomas S, Hoxha K, Tran A, Prendergast GC. Bin1 antibody lowers the expression of phosphorylated Tau in Alzheimer's disease. *J. Cell. Biochem.* 2019b; 120: 18320-18331.

Thomas S, Mercado JM, DuHadaway J, DiGuilio K, Mullin JM and Prendergast GC. Novel colitis immunotherapy targets Bin1 and improves colon cell barrier function. *Dig. Dis. Sci.* 2016; 61: 423-432.

Thomas S. An engraved surface induces weak adherence and high proliferation of nonadherent cells and microorganisms during culture. *Biotechniques* 2020; 69:113-125.

Ungaro R, Mehandru S, Allen PB, Peyrin-Biroulet L, Colombel JF. Ulcerative colitis. *Lancet* 2017; 389:1756-1770.

Wechsler-Reya R, Sakamuro D, Zhang J, Duhadaway J, Prendergast GC. Structural analysis of the human BIN1 gene. Evidence for tissue-specific transcriptional regulation and alternate RNA splicing. *J Biol Chem.* 1997; 272: 31453-31458.

Wickham H. *ggplot2: Elegant Graphics for Data Analysis*. Springer-Verlag New York, 2016.

Fig. 1

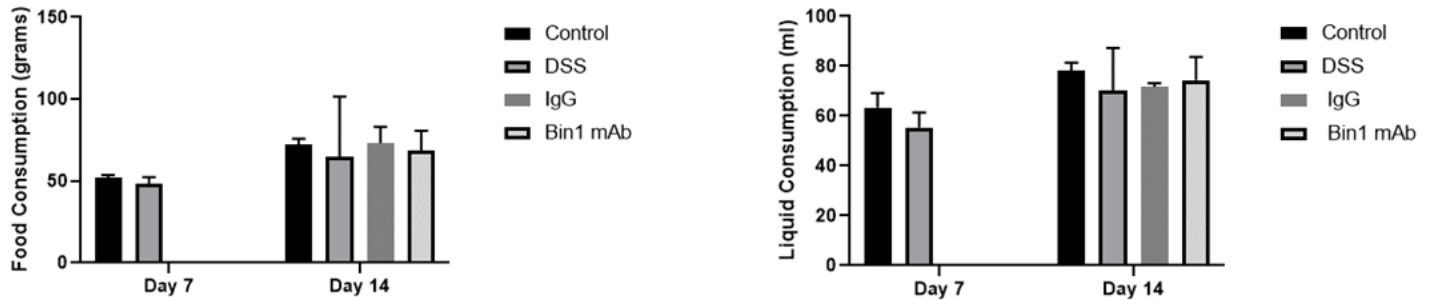


Fig. 1. No difference in food or liquid consumption between treatment cohorts.

Fig. 2

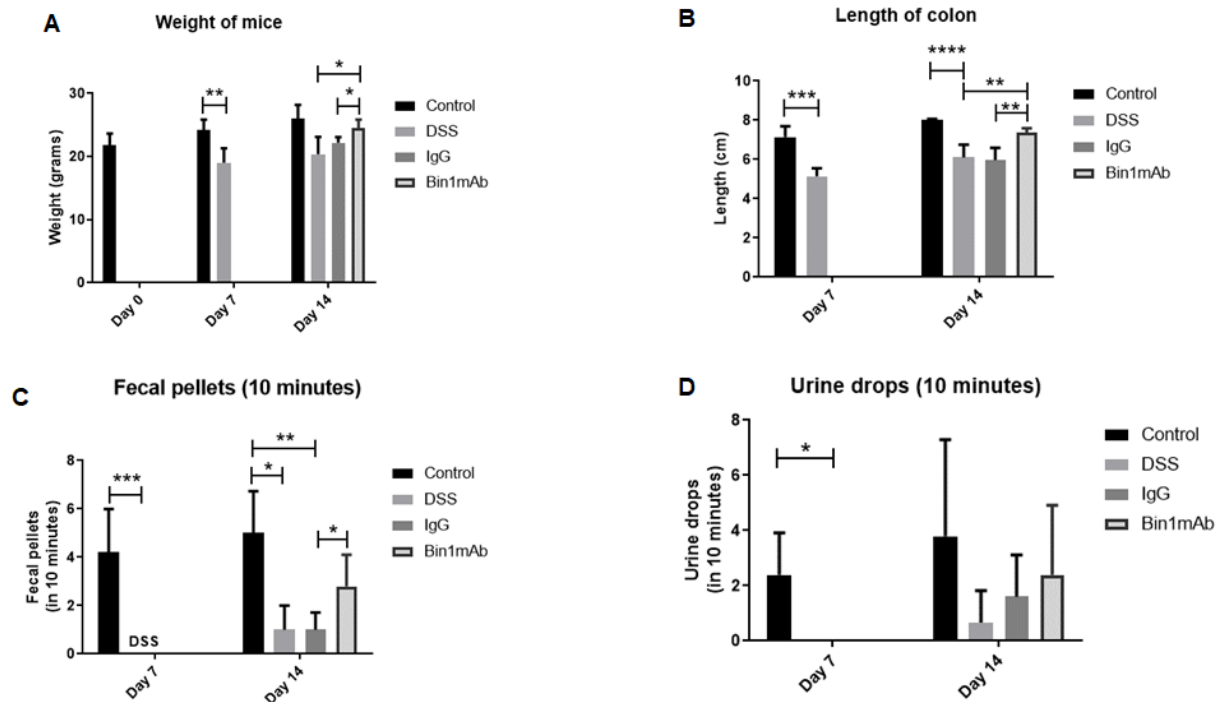


Fig. 2. Phenotypic effects of Bin1 mAb treatment in DSS-treated mice. There was a change in weight of mice, length of colon and the amount of fecal pellets after treatment with Bin1 mAb after subjecting to DSS treatment (*P<0.05, **P<0.01, ***P<0.001, ****P<0.0001, as determined by t test). Bin1, bridging integrator 1; DSS, dextran sodium sulfate; mAb, monoclonal antibodies

Fig. 3A

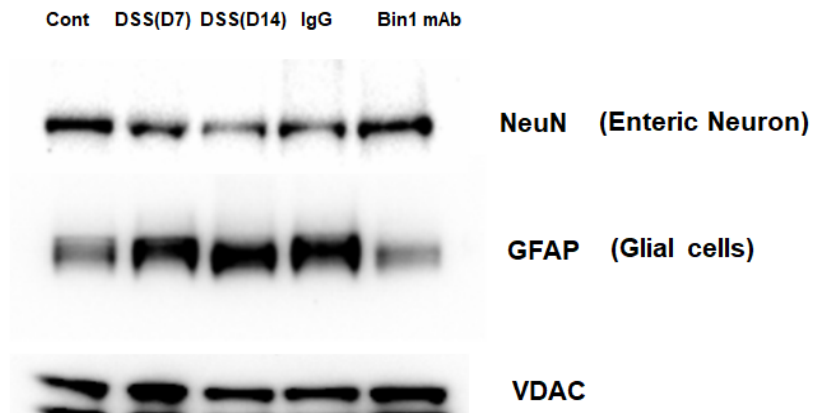


Fig. 3A. Effect of Bin1 mAb treatment on neuronal and glial abundance in the gut of UC mice. Bin1 mAb treated mice had high expression of NeuN and low expression of GFAP as determined by western blotting. NeuN, neuronal nuclear protein; GFAP, glial fibrillary acidic protein; VDAC, voltage-dependent anion channel

Fig. 3B

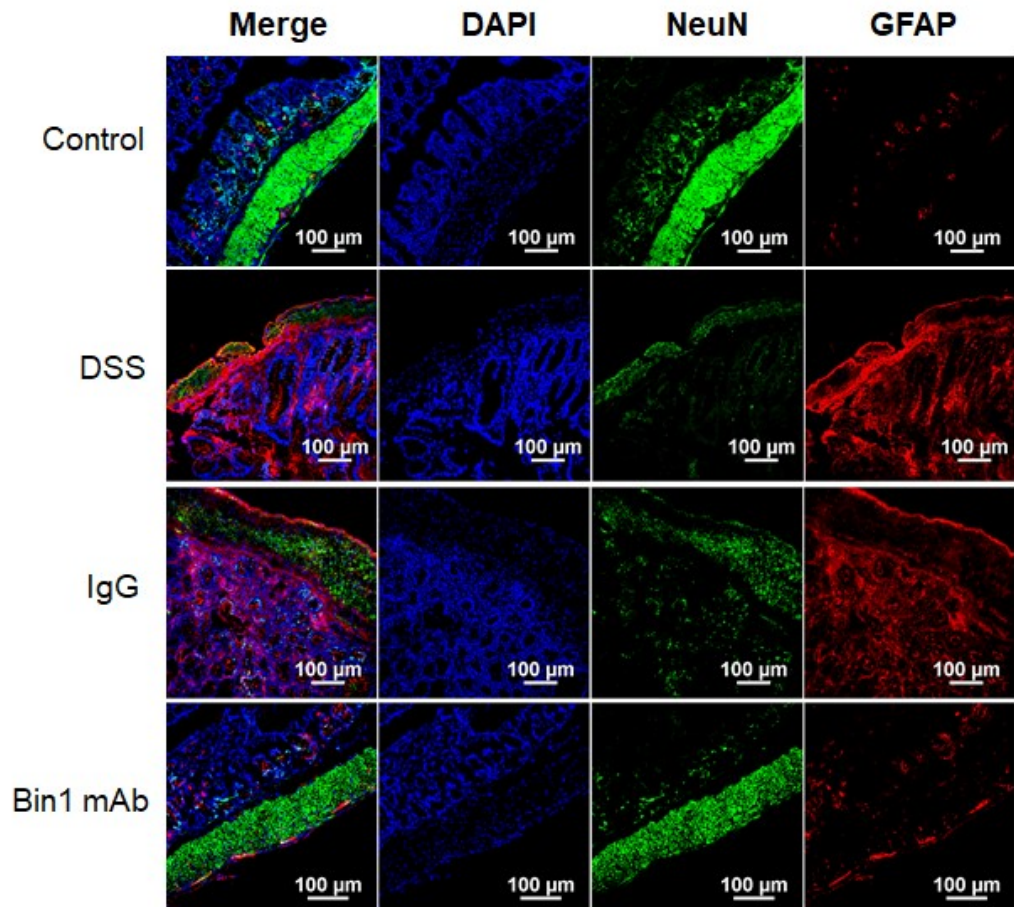


Fig. 3B. Effect of Bin1 mAb treatment on neuronal and glial abundance in the gut of UC mice as determined by confocal microscopy. Bin1 mAb treated mice had high expression of NeuN and low expression of GFAP.

Fig. 4A

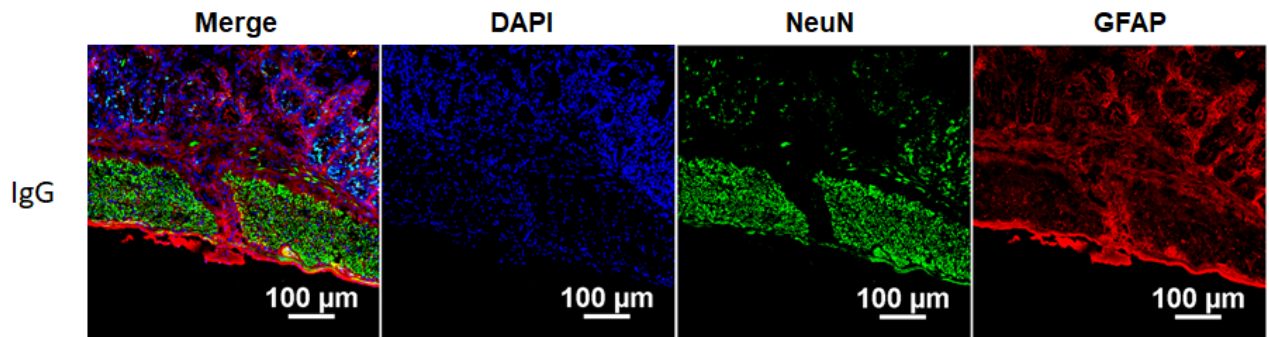


Fig. 4A. The muscularis of the colon is not a continuous entity. It has openings (*anigma*) that transport glial cells (stained with GFAP), which protect the enteric neurons.

Fig. 4B

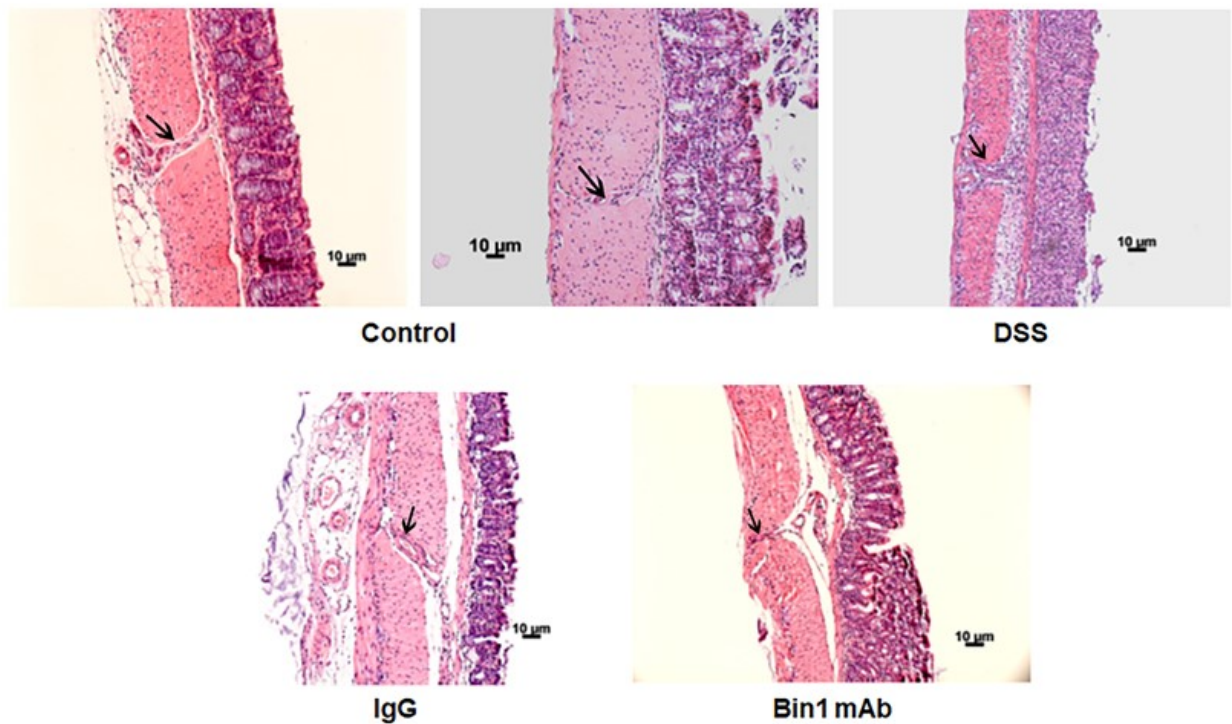


Fig. 4B. H and E staining of the mouse colon showing that muscularis is not a continuous entity. The muscularis of the colon is punctuated with openings (*anigma*).

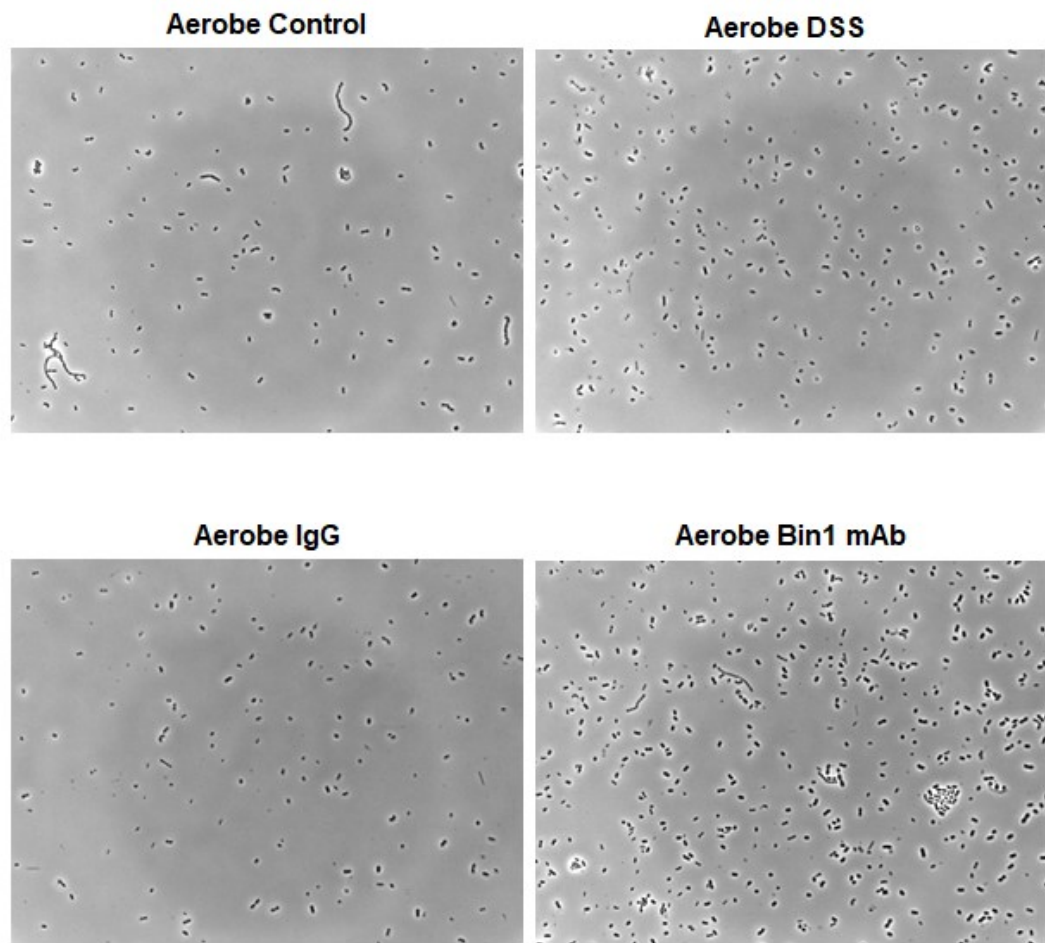
Fig. 5A

Fig. 5A. Aerobic culture of microorganisms show that the phenotype of Bin1 mAb treated mice has bacteria similar to the control (Phase contrast, 500X).

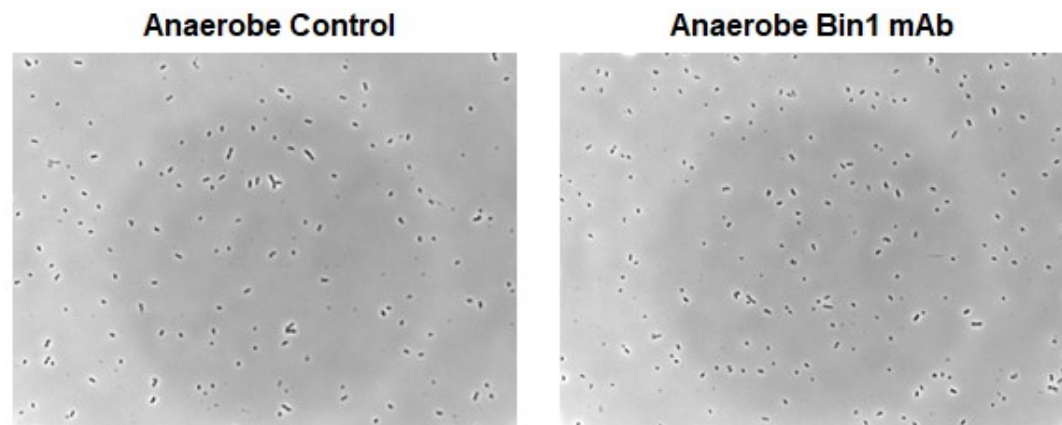
Fig. 5B

Fig. 5B. Anaerobic culture of microorganisms from fecal pellets were slow growing. There was no change in phenotype of the microorganisms between treatments (Phase contrast, 500X).

Fig. 6

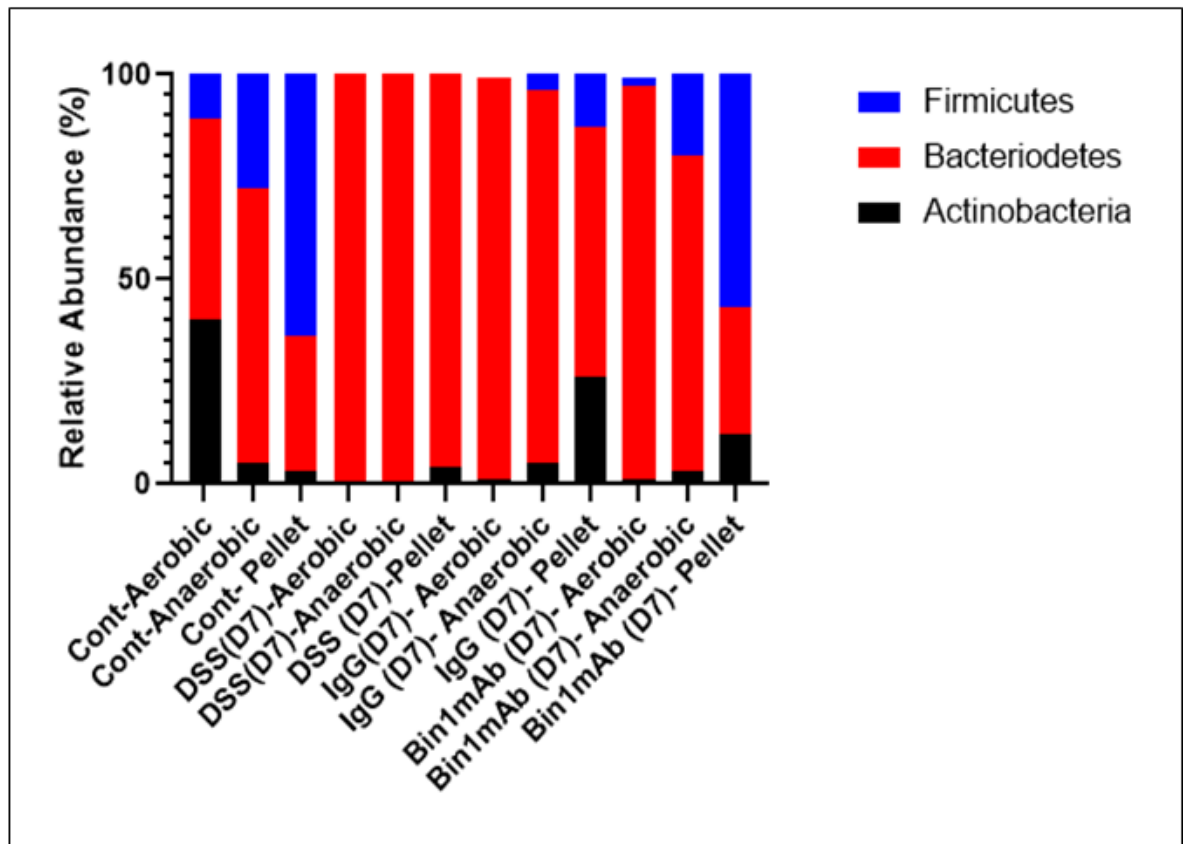


Fig.6. Microbiome sequencing by 16S rRNA shows the lack of Firmicutes during UC in the fecal pellet or when cultured in a biosimulator under aerobic and anaerobic conditions. The level of Firmicutes improved during treatment with the Bin1 mAb.

Fig. 7

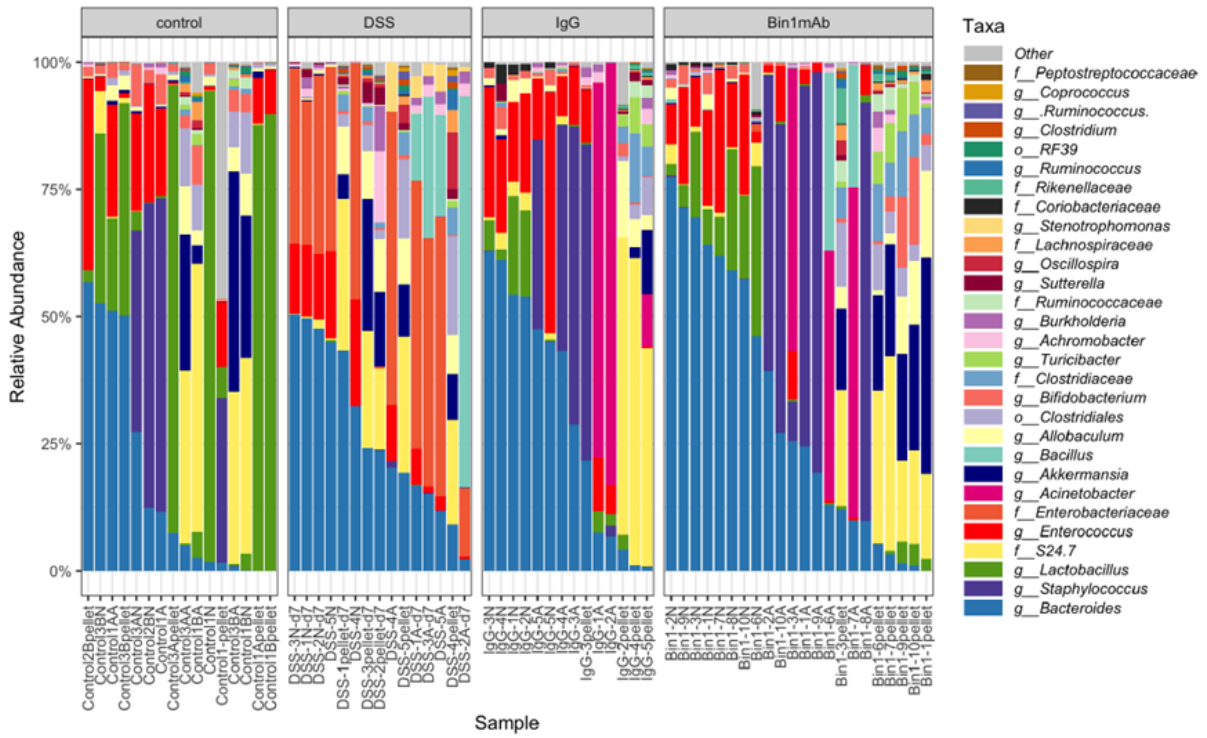


Fig. 7. Individual microbiome sequencing of fecal pellets of mice from different treatment conditions. The bacteria of the genus *Lactobacillus* is totally absent in the UC mice.

Fig. 8

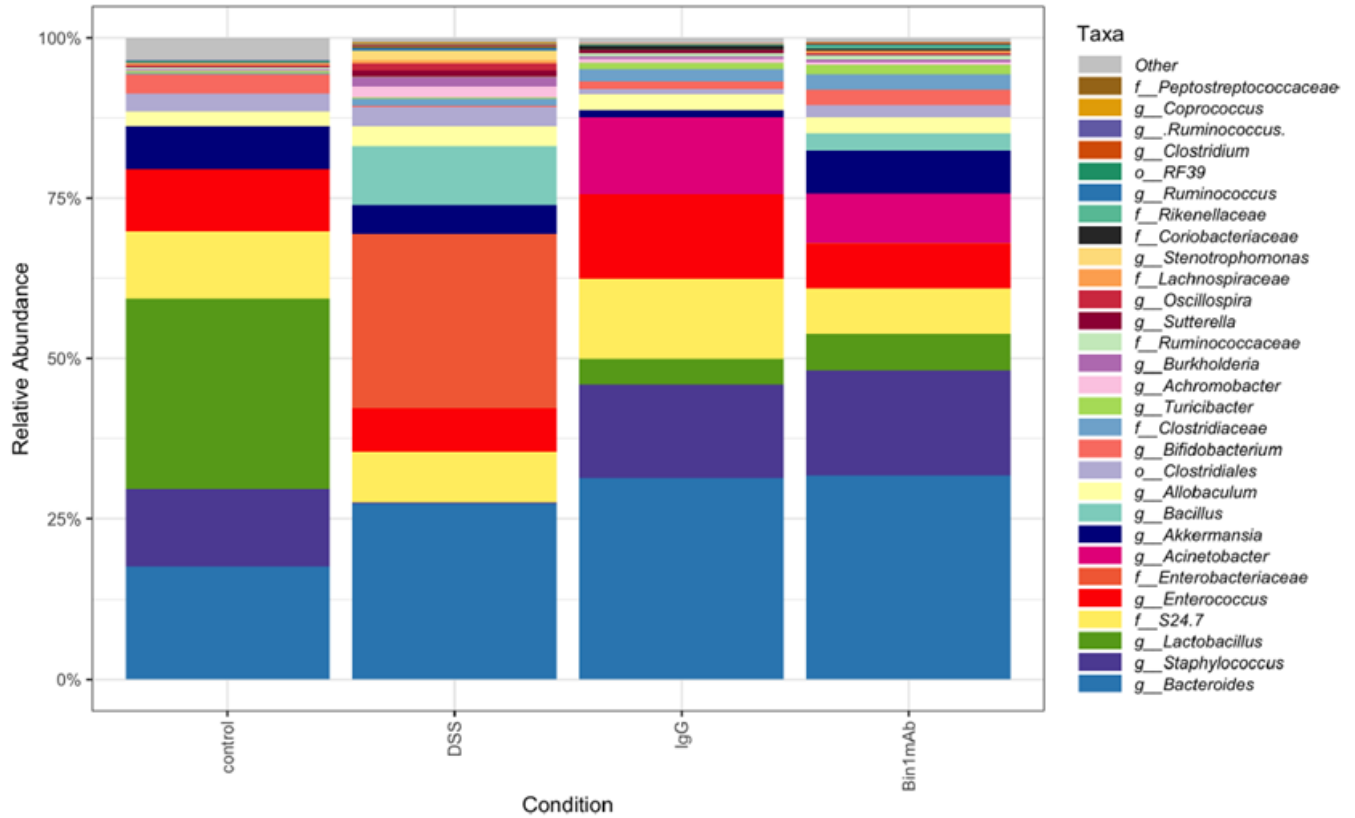


Fig. 8. The relative abundance of the microbiome in the pooled fecal pellets of mice from different treatment conditions. The bacteria of the genus *Lactobacillus* is totally absent in the UC mice.

Fig. 9

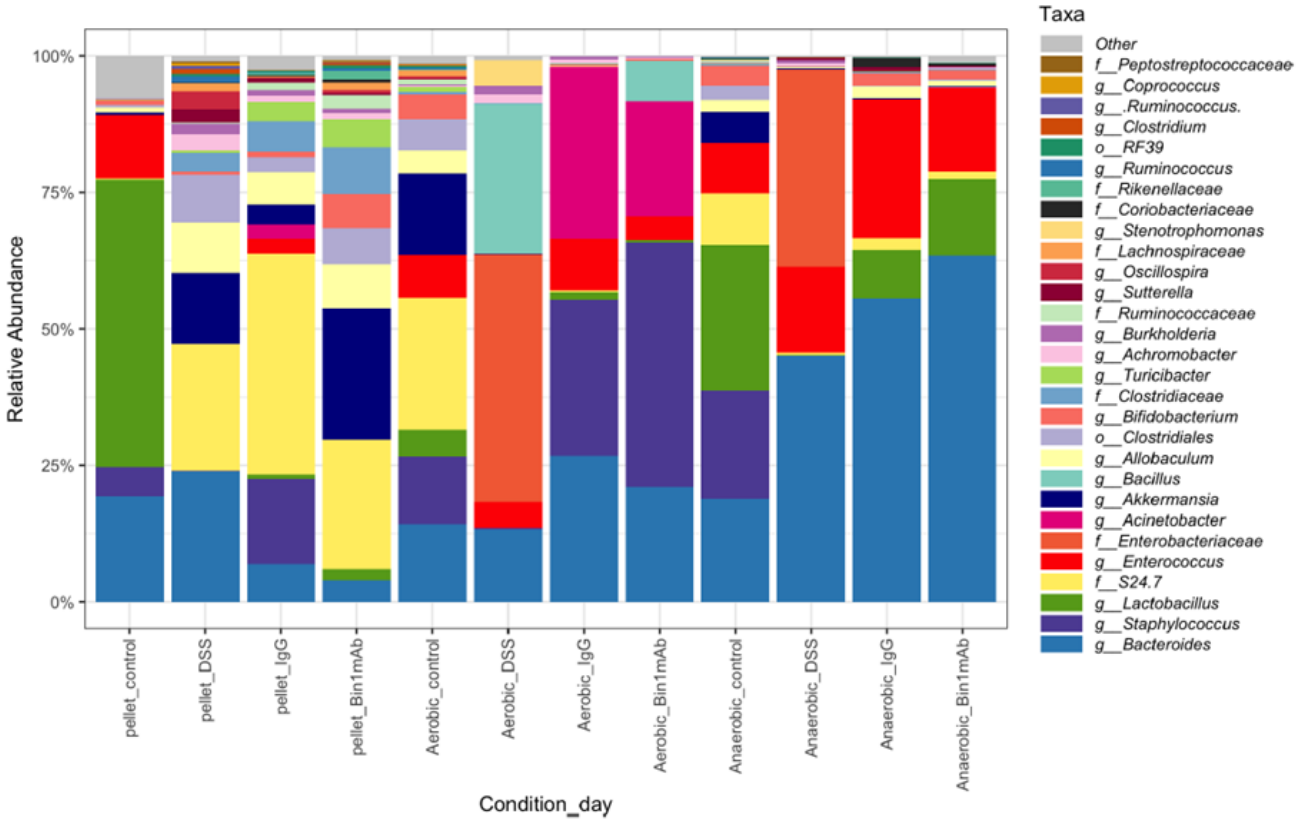


Fig. 9. The relative abundance of the microbiome of the fecal pellets of mice from different treatment conditions. The bacteria of the genus *Lactobacillus* is totally absent in the UC mice. The UC mice is enriched in *Enterobacteriaceae*.

Table 1. Expression of important microorganisms in animal models of UC before and after Bin1 mAb treatment

Microorganisms	Pellet				Aerobic				Anaerobic			
	Cont	DSS	IgG	Bin1 mAb	Cont	DSS	IgG	Bin1 mAb	Cont	DSS	IgG	Bin1 mAb
Bacteroides	3	3	2	2	3	3	3	3	3	4	5	5
Staphylococcus	2	0	3	0	3	0	4	5	4	0	0	0
Lactobacillus	5	0	1	2	2	0	1	1	4	0	2	3
S24-7	0	4	5	4	4	0	1	0	3	1	2	2
Enterococcus	3	0	2	0	3	2	3	2	3	4	4	4
Enterobacteriaceae	0	0	0	0	0	5	0	0	0	5	0	0
Acinetobacter	0	0	1	0	0	0	4	3	0	0	0	0
Akkermansia	0	3	2	4	3	0	0	0	2	0	0	0
Bacillus	0	0	0	0	0	4	0	2	0	0	0	0
Allobaculum	1	3	2	3	2	0	0	0	1	0	1	1
Clostridiales	0	3	1	2	2	0	0	0	1	0	0	0
Bifidobacterium	0	1	1	2	2	0	0	0	2	0	1	1
Clostridiaceae	0	1	2	2	0	0	0	0	0	0	0	0
Turicibacter	0	1	2	2	0	0	0	0	0	0	0	0
Achromobacter	0	2	1	1	0	1	0	0	0	1	0	0
Burkholderia	0	1	1	1	0	1	1	0	0	1	0	0
Oscillospira	0	2	0	0	0	0	0	0	0	0	0	0
Sutterella	0	2	1	0	0	0	0	0	0	0	1	0
Stenotrophomonas	0	0	0	0	0	2	0	0	0	0	0	0
Coprococcus	0	1	0	0	0	0	0	0	0	0	0	0

Absent: 0
 Very Low: 1
 Low: 2
 Moderate: 3
 High: 4
 Very High: 5